

# **Comparison and Verification of Experimental and Numerical Models for the Prediction of the Efficiency of Engine Noise Shields**

**F. Augusztinovicz, P. Sas and F. Penne**  
Katholieke Universiteit Leuven, Mech. Eng. Dept.  
Leuven, Belgium

---

## **ABSTRACT**

The paper summarises the results of those investigations, aimed at adopting and verifying numerical prediction methods for the determination of the efficiency of engine sound shields. An extended measurement series was conducted on simple engine simulators both under free field conditions and with engine shields of different complexity around the engine mock-up. The effect of the various shield configurations was expressed in terms of narrow or 1/3 band insertion loss spectra for single points or averaged along plane surfaces. Parallel to the experiments a number of detailed Boundary Element calculations were performed. The obtained results were compared and critically evaluated, and the calculation procedures refined.

It was found that the efficiency of the sound shield is determined by a large number of parameters and complex interactions between the radiator surface / air gap / sound shield system. These effects which often remain latent for traditional calculation methods can be sufficiently well predicted by using the BE method if rigid shields are assumed. Due to the relatively large apertures encountered in engine shields in practice, the assumption of a rigid shield is fully justified; calculations for sound shields provided with absorbent lining are still in progress during the preparation of this manuscript. The relative IL quantity can usually be calculated more accurately than the absolute sound field descriptors (with and without the shield) themselves.

---

## **1. INTRODUCTION**

Due to the noise characteristics of the currently manufactured diesel engines and the internationally standardised measuring methods of the type approval tests, the pass-by levels of heavy trucks are usually determined by the engine noise (ref. 1). Consequently, the noise level emitted by the vehicle can only be reduced to the required level if the powertrain is equipped with an appropriately tailored close-fitting sound shield or a partial enclosure. In order to comply with the recently tightened European rules (ref. 2, to be put into force as from 1995), vehicle manufacturers need reliable but affordable computational tools to enhance their design and optimisation process while designing these enclosures. However, no classical analytical methods seem to be appropriate for predicting the performance of real-life enclosures. Earlier surveys have shown that the accuracy of the methods relying on plane wave models is often not satisfactory (ref. 3 to 5; a good recent summary can be found in ref. 15). Using other methods, such as those based on classical room theory (ref. 6), on a modal approach (ref. 7) or on diffraction calcu-

lations (ref. 8), a number of simplifying assumptions are required, the prediction is usually poor and the useful frequency band is often limited.

Up-to-date acoustic prediction methods have the potential to be useful for sound shielding prediction applications. Numerical, mainly BEM calculations, have been proven to provide good results for some simple cases, obviously mainly for the lower frequencies (ref. 9 to 11). However, the necessary size and complexity of the models can be prohibitive and the useful application range of the FEM-BEM techniques for real-life engine/shield systems still has to be explored. Asymptotic or statistical methods might be attractive alternatives for the high-end frequencies (ref. 12,13) because of their relative simplicity and low computational demands, even if they are insensitive to the relative position of important partial noise sources and apertures; a design parameter which is often a decisive factor determining the performance of the whole enclosure.

In order to establish the applicability and the practical limitations of these advanced techniques for the engine sound shielding problem, an extensive study consisting of parallel calculations and verification measurements was initiated in the framework of a European project (BRITE-EURAM Research Project PIANO). The preliminary results of these investigations, dealing with the development of a simple test structure and some early BEM sound field calculations, have already been published (ref. 17). The reaction of a simple sound shield on the overall radiation from the source was treated in another paper (ref. 18). The aim of this publication is to summarise the applied methods and the obtained results of numerical predictions and verification measurements for the determination of the insertion loss (IL) of various sound shields around simple mechanical engine simulators. Note that further investigations and full-scale verification experiments with real-life truck engines are in preparation.

---

## 2. SIMULATION EXPERIMENTS

The final aim of the work is to adopt various techniques for the given industrial problem and to explore their practical limitations. The developed calculational scheme should enable industrial designers to predict the expected effect of various shield designs, given the noise radiation characteristics of the engine in sufficient details. While keeping this final goal in mind, it seemed to be more efficient to conduct the experiments on simple engine simulators in the course of the tool development phase.

The experimental set-up developed for the BE work (to be operational at lower frequencies) consists of a mechanical mock-up as engine simulator, surrounded by a modular sound shield system. Details of this set-up can be found in (ref. 19) and Sections 2.1 and 2.2 below.

### 2.1. Engine simulator

The requirement, mainly determining the development of the test source to be used for BE verification experiments, was that while retaining some resemblance to a real-life engine block, it should be sufficiently simple and amenable to numerical treatment. Its design was constrained by the trade-off between the required frequency band of the numerical predictions on one side and by the computing effort needed for the calculations on the other. As known from the literature of engine noise (see e.g. ref. 14), there are important noise components and therefore the upper frequency limit of the predictions should range up to 3 kHz. Considering the necessary

spatial resolution of the acoustical numerical modelling as well as the typical physical dimensions of a heavy diesel engine, one eventually ends up with as many as some 14 000 elements on the surface of the engine alone (not counting the necessary elements for the shield which can possibly be even much higher). This spatial resolution was found to be unaffordable and unnecessary for the exploration phase of the work.

Instead, it was decided to build a relatively small, welded steel rectangular mock-up structure which, in turn, has similar modal frequencies like a real-life engine. For the sake of realistic modal frequencies a number of trial calculations were performed on structures of various sizes, thicknesses and bulkhead configurations by using a standard structural FE software package (MSC NASTRAN).

Finally, all these considerations have resulted in a welded steel box of dimensions 400 mm x 300 mm x 150 mm, plate thickness 5 mm, with one symmetric bulkhead inside and a similar plate on top but no rigid plate below, thus leaving the bottom edges of the structure freely vibrating. According to FE calculations this structure has 14 vibration modes between 300 Hz and 1000 Hz. This modal behaviour of the source seemed to be sufficient to simulate engine block vibrations, even if the vibration of real engines is composed of much higher numbers of forced harmonic components in this frequency range.

The free bottom solution approximates the vibration of the usual engine blocks, but could cause unwanted modelling complexity. The real box is therefore closed on the bottom by using a thick PVC plate, connected airtight by using a thick, resilient layer of silicone rubber. For more details about the source and its characteristics see (ref. 17 and 19).

The development of the scale model was completed by performing an experimental modal analysis (EMA) test. The normal accelerations were measured in a 40 mm x 30 mm mesh on the outer surface of the structure, resulting in 296 measurement points. The FRFs, referenced to the input force provided by an electrodynamic shaker, were calculated and stored for later use, both as input data for modal extraction by using standard EMA methods as well as direct inputs (velocity boundary conditions) for the acoustic predictions. The measurements and the subsequent modal analysis were performed by means of an LMS CADA-X measurement system; a typical FRF is shown in Fig. 1.

It is worth to note here the low structural damping of the test structure. One can anticipate that the radiated sound field will show high variance (both in space and in frequency), caused by the low modal damping and modal overlap. As will be shown below, this is indeed the case.

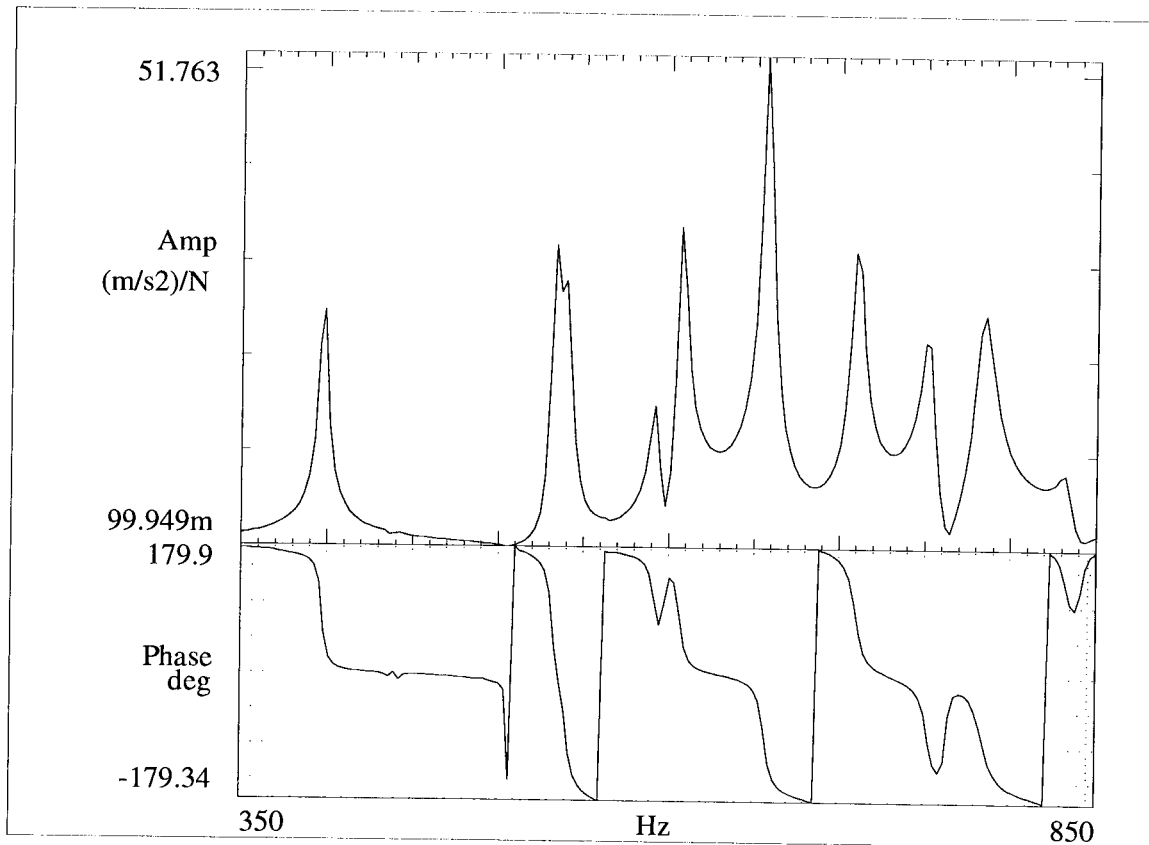


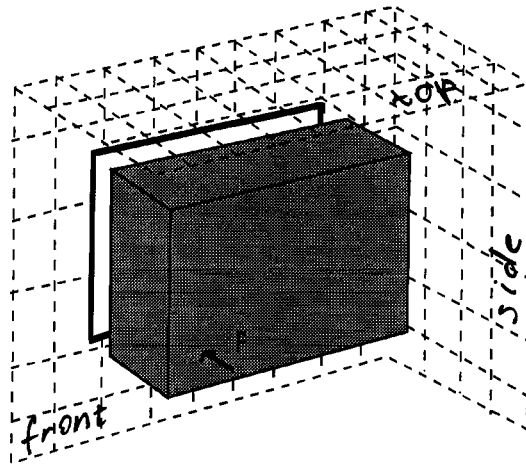
*Fig.1. A typical structural FRF of the mechanical mock-up  
(surface acceleration referenced to unit input force)*

## 2.2. Sound shields

Two essentially different shields were applied in the course of the simulator measurements: a simple steel plate, having identical dimensions as the largest side panel of the test source, and a modular shield system, being able to accommodate a wide range of various shielding elements around the source. The steel plate (with a thickness of 3 mm, provided with 10 mm thick damping material) was placed at 50 mm distance from the source (see Fig. 2.a).

The basis of the modular set-up is a rigid steel frame fixed to a wooden plate onto which various shield elements such as thick, rigid steel plates, flexible plastic or aluminium plates can be screwed. The plates can be untreated or covered with sound absorbing lining, with or without apertures. Some of the results (both experimental and calculational) refer to a configuration where the two smallest sides of the modular shield are left open. This combination, aimed at modelling a real-life engine shield which is very often open in front and at the back to allow good cooling, will be referred to as a tunnel-type shield below (see Fig. 2.b). The outer dimensions of the supporting frame are chosen such that the distance between the vibrating surfaces of the source and the shielding plates is everywhere 75 mm.

a)



b)

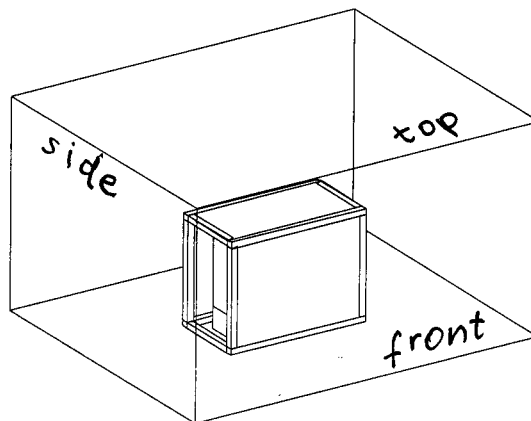


*Fig. 2. Shields and field point meshes in various experiments.  
a): plate shield, b): tunnel shield*

### 2.3. Acoustic measurements

The effect of the sound shields was evaluated by measuring sound pressures and sound intensities in the measuring points with and without the shield. In order to be in accordance with the numerical calculations where the sound field was calculated for 1 N input force, the sound pressures were measured in terms of frequency response functions, referred to the input force measured by means of a force transducer. The excitation was ensured by an electrodynamic shaker, the used excitation signal was band limited random noise between 200 and 3000 Hz. All measurements were performed in a semi-anechoic room.

Some measurements were performed in discrete points selected along various plane field point meshes, other ones were done by using manual surface scanning along the same meshes. The meshes were defined to be parallel to the side walls of the source as shown in Fig. 2a; more details can be found in (ref. 18). The insertion loss was calculated as a function of frequency both in terms of sound pressures and intensities, in the classical way:

$$IL = 20 \log \left( \frac{P_{free}}{P_{shield}} \right) \quad (dB) \quad (2.1)$$

or

$$IL = 10 \log \left( \frac{I_{free}}{I_{shield}} \right) \quad (dB) \quad (2.2)$$

where  $p$  and  $I$  denote amplitudes, determined either in discrete points or spatially averaged along the relevant mesh. The subscript *free* refers to the case where the source radiates in free field while *shield* refers to the situation where the enclosure is present.

---

### 3. NUMERICAL PREDICTIONS

The peculiarity of the sound shielding problem is that at the same time it is both a radiation and a scattering problem. In order to allow for the presence of a thin, non-closed obstacle in the sound field radiated from a known, complex source, the variational BEM approach seems to be the most attractive selection. (Note that further investigations by using the FE method and wave envelope elements are also in progress.) The results reported herein have been obtained by using the software package SYSNOISE (ref. 20).

#### 3.1. Source description possibilities

An important advantage of using a simple and well described source mock-up lies in the fact that a number of conceivable source description methods can be easily compared. The available data base enabled us to perform comparative predictions under free-field conditions, by using the following approaches for the description of the source:

- a) coupled option (i.e. coupled vibro-acoustic behaviour), source described in modal coordinates using measured structural mode shapes; structural damping neglected;
- b) coupled option, source described in modal coordinates using measured structural mode shapes; structural damping included in the calculations;
- c) uncoupled option, source described in modal coordinates using measured structural mode shapes; structural damping included in the calculations;
- d) uncoupled option, source described by measured surface vibration data as directly imposed boundary conditions.

The calculated and measured sound field descriptors were compared in terms of intensity maps (amplitude vs. spatial coordinate, with the frequency as parameter) and intensity FRFs (amplitude vs. frequency, with the field point as parameter). The patterns of the obtained intensity maps were virtually identical (ref. 17). As one expects, however, the lack of damping yielded considerable deviations in the amplitudes, rendering the results inappropriate for relative IL calculations.

Viewing the high internal impedance of the applied source, it is rather plausible that the coupled option is not really necessary. The results of the calculations have justified the expectations: the difference between the surface displacement assuming and neglecting coupling is low (even though not negligible; mostly below and around 10 %) and the resonance frequencies

do not change more than 1 Hz either. Note that similar agreement was found with and without the plane sound shield and the calculations were backed by experiments, too. This means that the use of the same velocity boundary conditions is correct, both with and without the shield.

Comparing the calculated sound field descriptors, obtained by using modal coordinates (coupled calculation, damping included) and by using measured velocity patterns as boundary conditions, it was established that usually this latter approach yields the best agreement. Once again, this is in agreement with the expectations since omitting the two consecutive steps of modal extraction - modal synthesis necessarily improves the accuracy.

In view of these achievements one is tempted to draw the conclusion that the best method for the source description is the direct velocity boundary condition method. Nevertheless, some problems can be encountered. First of all, it is virtually impossible to perform a detailed surface vibration measurement series on a running engine which could yield the surface velocities of the whole engine with the required spatial resolution. The problem is hoped to be solved by using the equivalent power volume velocity method (ref. 16) rather than using directly measured surface vibrations. This method seems to be sufficiently robust, and its implementation for numerical calculations is in progress.

### **3.2. Calculation of the insertion loss**

Using the source description methods *b)* or *d)* as discussed above, the BE problem was solved by imposing zero velocities (rigid shield) or impedance boundary conditions (sound absorbing lining) along the numerical model of the shield, e.g. the one of the tunnel-type shield as shown in Fig. 3. With the first structural mode as lower and the BEM surface mesh resolution as upper frequency limit, the selected frequency bandwidth was 350 Hz to 1420 Hz with a step of appr. 3.8 Hz. During the post-processing phase the normal sound intensity components and the sound pressures were calculated in discrete points along the same field point meshes as used in the course of measurements. The sound intensity or sound pressure vs. frequency FRFs were directly calculated with and without the shield for selected discrete field points, or the FRFs were first averaged along various field point surfaces by using a separate, small user program. The Insertion Loss spectra were calculated in both cases by using Eqs. (2.1) and (2.2). A typical narrow-band sound intensity spectrum with and without the plane sound shield and the derived IL spectrum is shown in Fig. 4.



## SYSNOISE - SYSTEM FOR ACOUSTIC ANALYSIS

Rev 5.0 HP-UX 15-NOV-93

Radiator with velocity b. c., tunnel shield, hs -0.095 ,singular

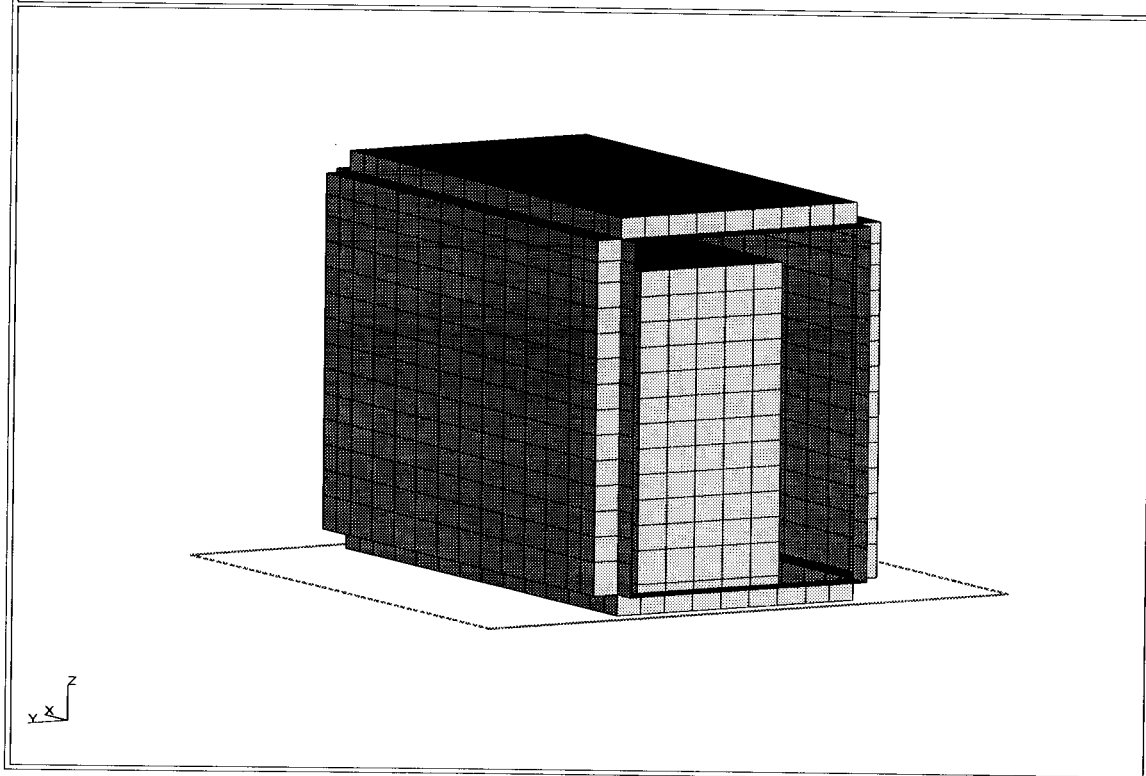


*Fig.3. The numerical model of the tunnel shield configuration*

## 4. DISCUSSION AND COMPARISON OF MEASURED AND PREDICTED INSERTION LOSS SPECTRA

The efficiency of the shield is evaluated in terms of IL spectra throughout this paper. Some typical sound field patterns with and without the plane sound shield have been published in (ref. 17). The detailed analysis of the effect of the shield on the radiation impedance and thereby on the radiated overall power of the source is discussed in (ref. 18).

### 4.1 Plane sound shield

The intensity spectra, measured with and without shield and averaged for the measurement plane #1 behind the shield are compared in Fig. 4.a. while the IL curve is depicted in Fig. 4.b. The evaluation of the IL vs. frequency curve shows how different the effect of the shield for various frequencies can be. For 399 Hz, 662 Hz and especially for the 755 Hz modal frequency of the structure the shield acts as a sound reducing element (as one can observe along the field point mesh lying behind the shield), but for 533 Hz and 714 Hz amplification rather than reduction is encountered.



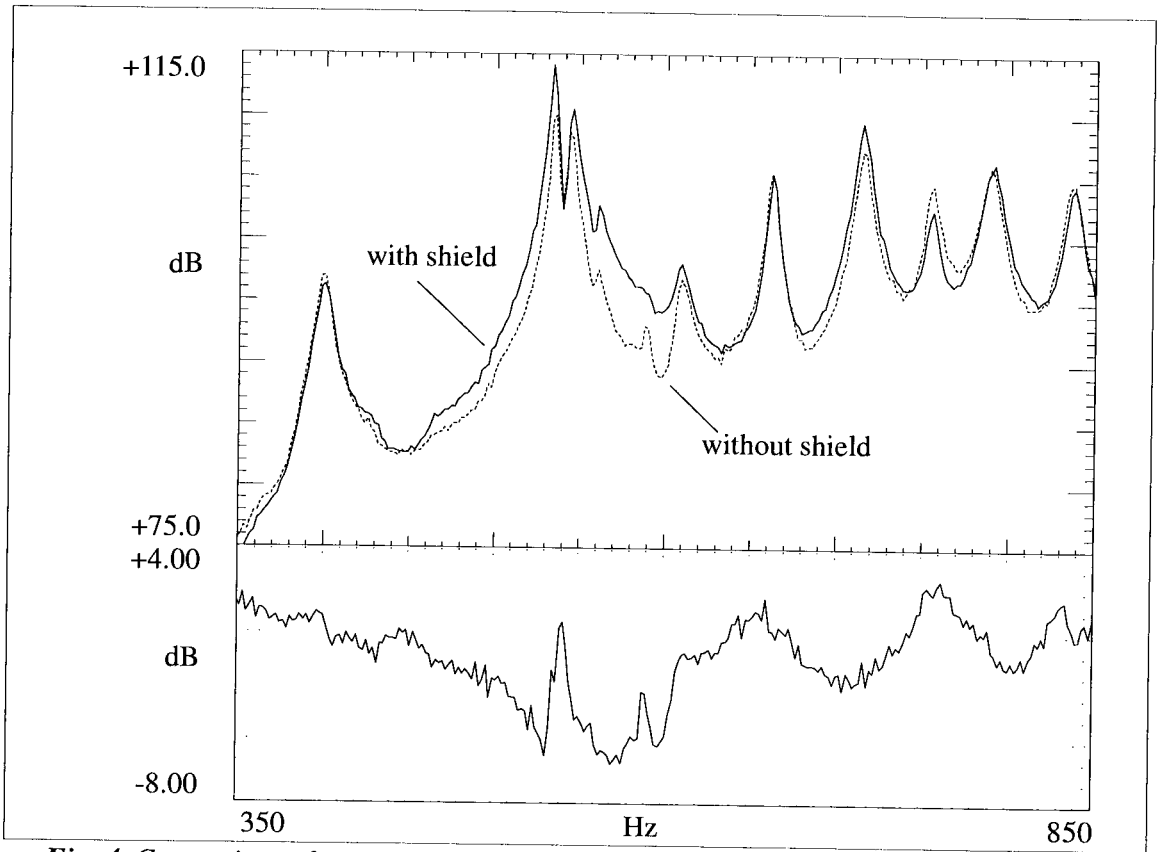


**Fig. 4.** Comparison of spatially averaged intensities, measured under free-field conditions and with rigid tunnel shield and the obtained narrow band IL spectrum

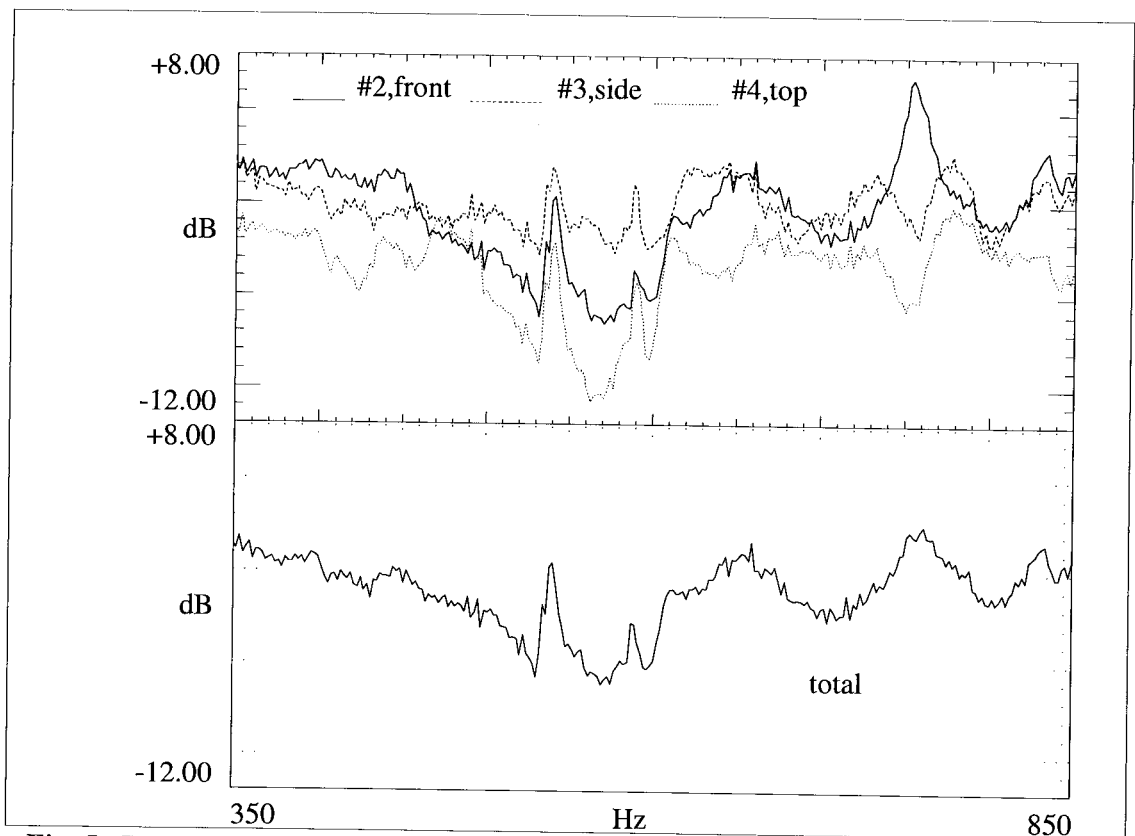


**Fig. 5.** Comparison of measured IL spectra of the plane sound shield, averaged for various meshes and for the whole measurement surface in narrow bands

The spatial variation of the insertion loss can be investigated by comparing the acoustic intensity levels, averaged over the three meshes depicted in Fig. 2.a as shown in Fig. 5. On the basis of these curves one can conclude that the shield modifies the power flow from the structure mainly towards the top of the structure, although a considerable amount of sound energy is propagating behind the shield, too. On the other hand, the shield not only redirects but also increases the radiated power in absolute terms. The latter effect is caused by the change in acoustic impedance due to the presence of the shield.

The accuracy of the prediction was first investigated by calculating the IL values for selected points and for some important modal frequencies of the structure by using the uncoupled variational approach. The agreement was not satisfactory: differences from 0 to 10 dB were found. (It is worth to note that the accuracy of the absolute predictions were in general worse, ranging up to 14 dB.) The analysis was repeated by averaging along the used field point mesh (#1), and the accuracy was considerably improved, see Fig. 6 below.

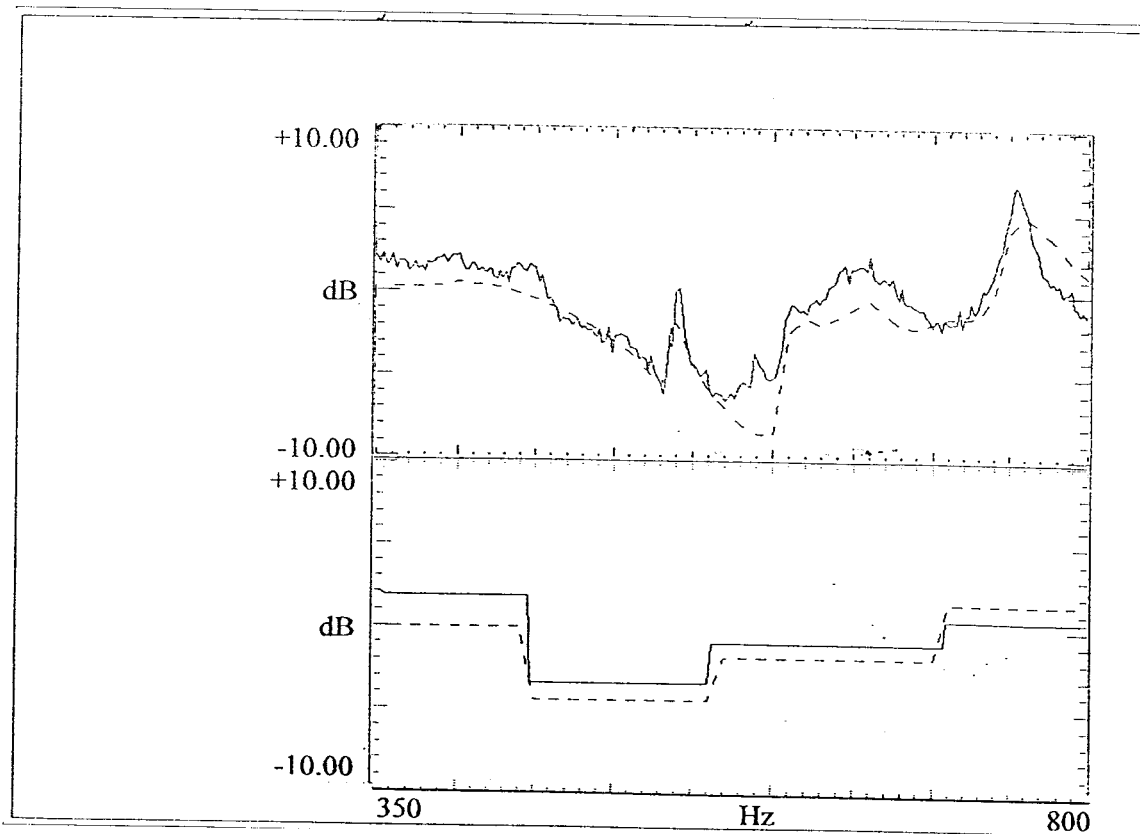


**Fig. 6:** Effect of the plane sound shield, spatially averaged along the front mesh. Comparison of measurements (solid line) with calculations (dotted line)

As one can see, the agreement is rather good with about 2 dB variation in the majority of the frequency bands (with slightly higher variations for the mid-frequencies, presumably caused by some flanking propagation from the shaker support). The differences are even lower if third-octave band spectra are compared (see Fig. 5.b.): maximum 1.5 dB variation was observed from 500 Hz upwards and less than 2 dB for the lowest band, 400 Hz. This means that in spite of the relatively inaccurate predictions of the absolute levels with and without the shield, its relative effect, i.e. the insertion loss can be predicted quite accurately.

## 4.2. Tunnel-type rigid shield

The experiments with the tunnel-type shield has revealed, that the sound field of the system is more irregular than it was the case with the plane shield, characterised by strong influence of constructive and destructive interferences. The effect of the shield can be discussed in full details on the basis of Fig. 7. where the measured insertion loss spectrum (diagram in the middle) is depicted together with the average structural FRF of the source (upper diagram) and an acoustic FRF of the gap in between the source and shield (lower diagram). The structural FRF, Fig. 7.a, was obtained by averaging all 296 structural FRFs used for the modal analysis test as described above, while Fig. 7c. depicts a sound pressure FRF, measured in the gap between the source and shield and referenced to the surface acceleration, sensed in the vicinity of the microphone.

The IL vs frequency curve shows a number of sharp local maxima and minima. Some of the maximum frequencies coincide with structural modes of the source, e.g. at 520, 750 and 1101 Hz, but other structural modes are accompanied with sharp dips in the IL spectrum (this is the case for 567 and 823 Hz). This contradictory behaviour could be explained by performing modal analyses for the relevant modal frequencies. For frequencies of those structural modes which are characterised by a clear out-of-phase motion (in the sense that an element of the front plate of the source moves *toward* the fluid while its mirror element on the back side moves just *away* from it, see on the left side of Fig. 8) a strong insertion loss increase can be observed. In these cases the tunnel shield apparently contributes to a better cancellation of radiation between the front and back side of the source (the shield "helps" the acoustic short-circuit to be more effective). For modes which behave just the other way, as shown for the mode at 567 Hz, the effect is the opposite, too. For "mixed" modes no such strong variation in the IL curve can be found. All these mean that the main operating mechanism of the rigid tunnel-type shield is to change the radiation from the source itself, instead of changing its propagation direction or reducing the amount of energy by dissipation. Note that the explanation is also true for frequencies in between the modal frequencies, as it has been proved by means of running mode analysis of the structure.

Some of the insertion loss dips cannot be explained this way, for example at 835 and 1220 Hz. For almost all these frequencies one can however find a local maximum, i.e. an acoustic mode, in the air gap between the source and the shield. The source can more effectively excite sound waves in the air for these frequencies (the numerical calculations show considerably higher radiation efficiency values), thus the insertion loss is reduced. Again, the shield changes the interaction between the source and its environment rather than to result in changes in the acoustic fluid only.

The prediction of the insertion loss was done by using the same methods as described above. The model size is considerably increased by the shield elements, resulting in rather long running times of the BE solution; the calculation of the IL spectra as shown below takes approx. 100 hours pure CPU time on a Hewlett Packard 715 type workstation.

The calculated IL spectrum of the rigid tunnel shield, averaged for the front plane of the field point mesh shown in Fig. 2b. is shown in Fig. 9. together with its measured counterpart. Apart from some sharp dips at certain frequencies, the accuracy of the prediction is rather good. These discrepancies are caused by singularities of the integral equation solution at frequencies equal or close to the eigenfrequencies of the interior space of the source model. Most of the time the radiation with the tunnel shield is seriously overestimated at these frequencies (accompanied by unreal values of the radiation efficiency), while the calculation for the free field case is correct or burdened with lower errors; in the end resulting in sharp IL decreases. The results of Fig. 9 has been obtained by using a number of highly absorbing overdetermination elements in the form of a rather large, contiguous surface within the source interior. Isolated elements were found to be much less effective; further calculations are in progress with even more absorption.

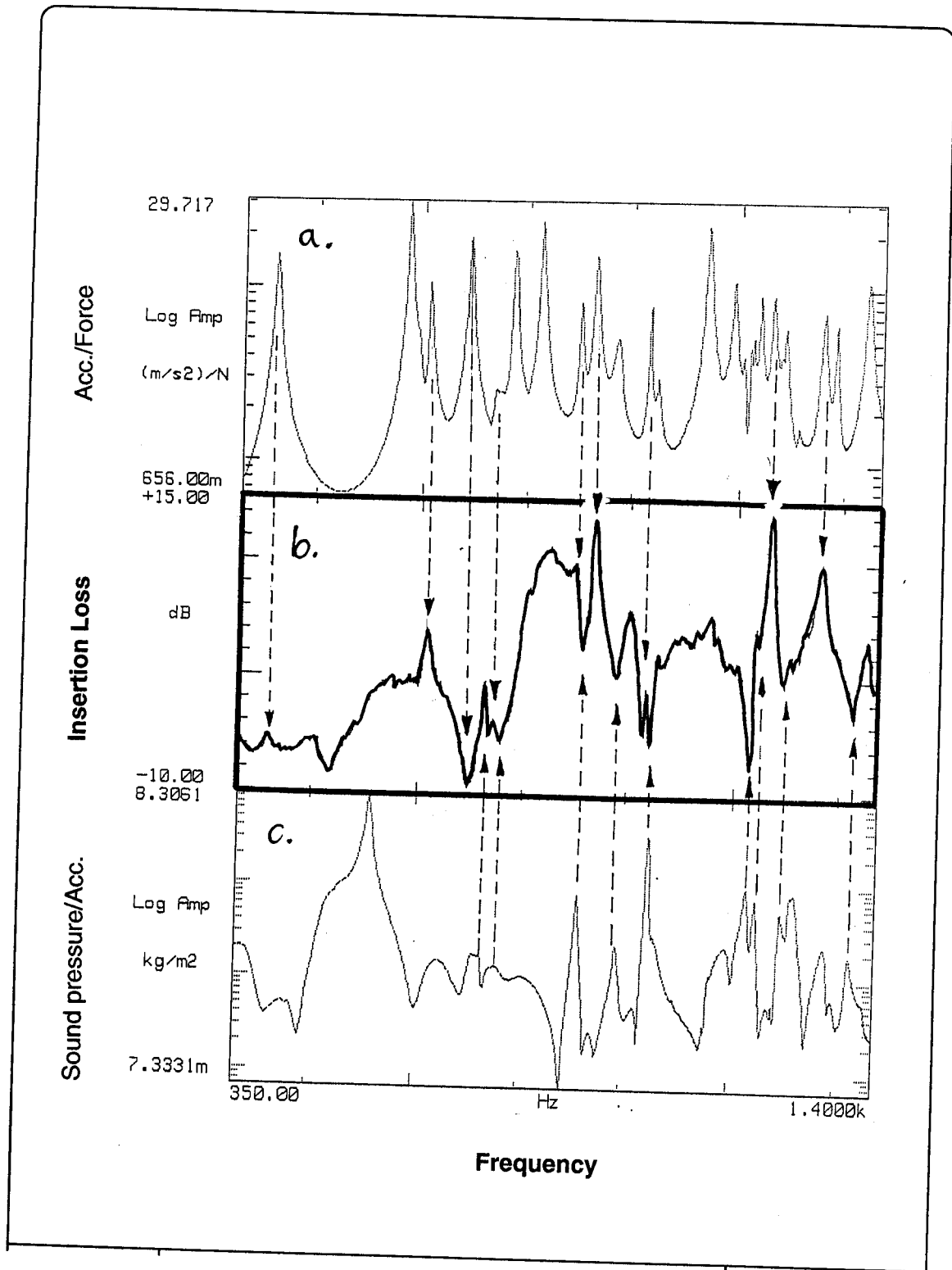


*Fig. 7. Comparison of the Insertion Loss spectrum (part b) to the structural (part a) and to the acoustical (part c) subsystem of the mock-up / air gap / sound shield transmission (further explanation in the text)*

**Mode shapes which are accompanied by IL maximum**

**Mode shape which is accompanied by IL minimum**

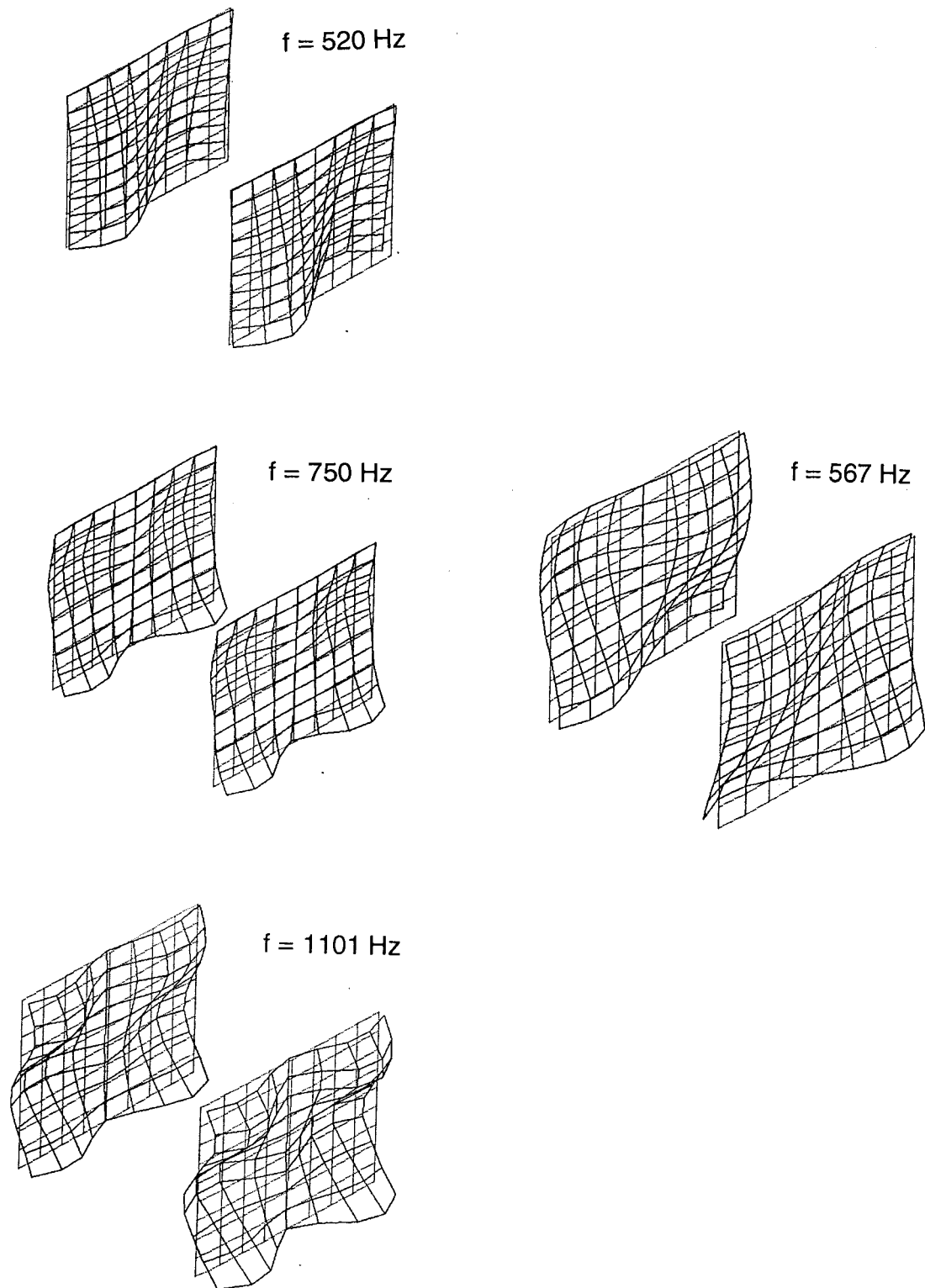


**Fig. 8.** Comparison of various structural mode shapes of the source mock-up

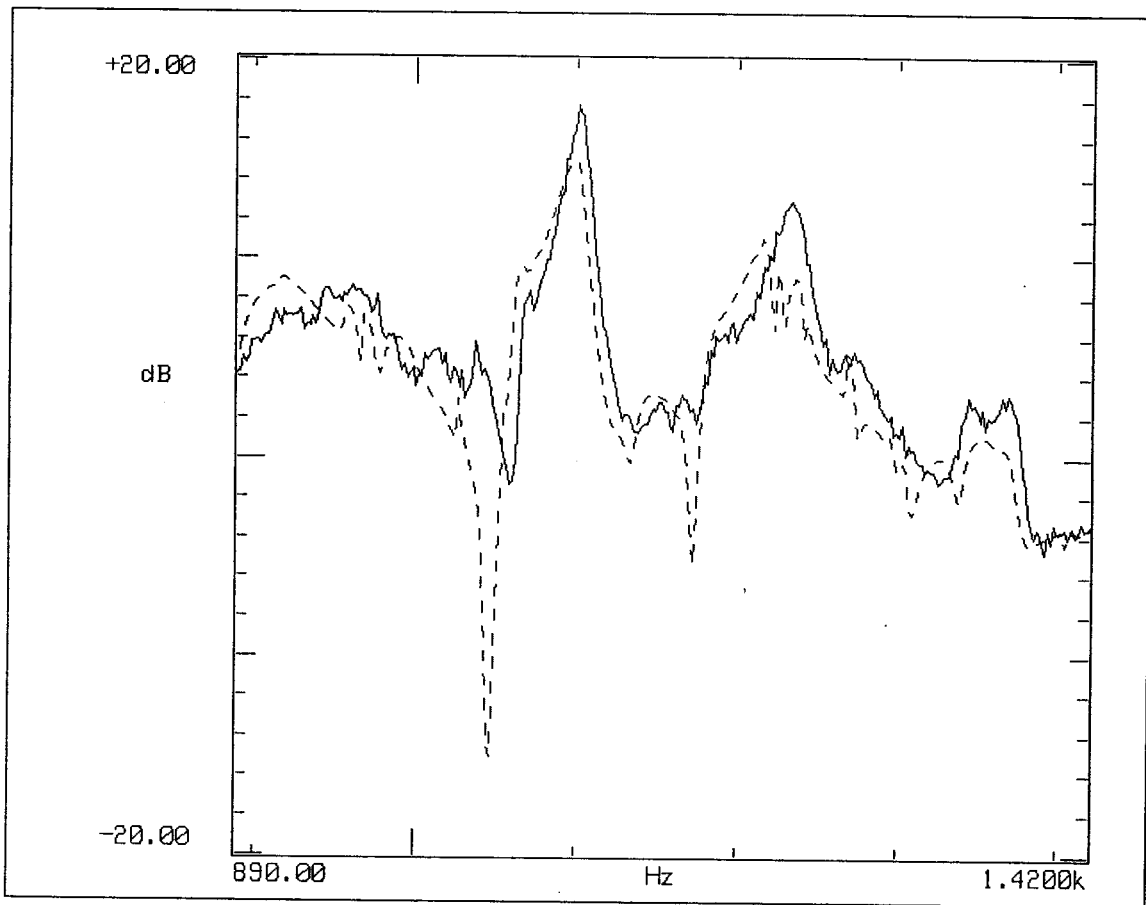


**Fig. 9.** Comparison of the measured (full line) and predicted (dashed line) Insertion Loss of the rigid tunnel-type shield

---

## 5. SUMMARY AND MAIN CONCLUSIONS

By means of simple mechanical and electroacoustic mock-ups and various shield configurations, parallel sound field measurements and calculations were performed applying the Boundary Element and the Statistical Energy Analysis method. The sound field was described in terms of narrow and/or third-octave band sound pressure and sound intensity spectra, determined in discrete points or along various field point meshes. Insertion loss (IL) curves were calculated. The effect of the shield was evaluated by means of IL spectra determined in single points and averaged along various measurement surfaces.

The most important conclusions are the following:

- The sound field of the applied mechanical engine simulator can be predicted with sufficient accuracy by means of uncoupled variational BEM approach if measured structural vibration data are used as source input, either in the form of extracted structural modes or as directly imposed velocity boundary conditions. In case of modal coordinates, special care has to be taken to input accurate modal damping values in a correct way. Using the surface velocity data as directly imposed velocity boundary conditions usually yields the best estimation of the sound field.
- It has been shown that the surface vibration of the applied mechanical structure is not influenced by fluid-structure interactions (caused e.g. by the presence of the shield), thus the use of a coupled calculation scheme is not required. This achievement justifies the use of the same surface vibration data set both for the free field and the shield case.
- It has been shown both experimentally and numerically that in spite of its relatively small size (both with respect to the wavelength in air and to the size of the source), a single plane sound shield can considerably change the radiation of the source. Besides the increase, energy redirection also takes place, accompanied by a strongly space-dependent insertion loss.
- It has been shown both experimentally and numerically that the influence of a close-fitting rigid shield on the insertion loss is mainly determined by complex interactions between the source and its acoustic environment.
- This insertion loss of various rigid shields could not be predicted with sufficient accuracy by using coupled variational BEM in single field points, but averaging along a field point mesh reduced the deviations considerably and thus resulted in acceptable estimations. The accuracy of the (relative) IL prediction is better than the accuracy of the (absolute) field prediction itself.
- The applied numerical approach leads to singularities for frequencies equal or close to the eigenfrequencies of the source model interior which are difficult to differentiate from structural radiation peaks. These singularities could be reduced (but not yet fully avoided) by putting a relatively large number of highly absorbing overdetermination elements in the numerical model.

---

## ACKNOWLEDGEMENT

The work reported herein was performed in the framework of the EC Brite/Euram Research Project PIANO (under contract BRE2-0210). The project is supported by the Directorate-General for Science, Research and Development of the Commission of the European Community what is gratefully acknowledged.

---

## REFERENCES

1. Drewitz, H. and Stiglmaier, M.: **Development of a capsule fixed to the engine of trucks of 6 to 17 t permissible gross vehicle weight**  
*Proc. Inter-Noise 90* (Ed. H.G. Jonasson), Göteborg, 13-15 August 1990, Vol. I. 489-492.p.
2. **Richtlijn 92/97/EEG van de Raad tot wijziging van Richtlijn 70/157/EEG**  
*Publikatieblad van de EG*, Nr. L 371, 19 december 1992, blz. 1.
3. Jackson, R.S.: **Some aspects of the performance of acoustic hoods**  
*J. Sound Vib.*, 1966, Vol.3. No.1. 82-94.p.
4. Junger, M.C.: **Sound transmission through an elastic enclosure acoustically closely coupled to a noise source**  
ASME Paper No. 70-WA/DE-12 (1970)
5. Tweed, L.W. and Tree, D.R.: **Three methods for predicting the insertion loss of close-fitting acoustical enclosures**  
*Noise Control Engineering*, 1978, Vol. 10. No.2. 74-79.p.
6. Mhango, A.J. and Petrie, A.M.: **The application of a modified room acoustic equation for the prediction of insertion loss of a close-fitting enclosure**  
*Proc. Inter-Noise 84*, 377-380.p.
7. Hillarby, S.N., Shen, Y. and Oldham, D.J.: **The performance of acoustic enclosures**  
*Proc. Inter-Noise 83*, 335-338.p.
8. Sung, Y.C.C. and Lalor, N.: **The prediction of engine noise reduction by using shields and partial enclosures and the optimization of their design**  
*Proc. IME Int. Conf.*, Birmingham, Paper C29/88 (1988) 117-122.p.
9. Terai, T.: **On calculation of sound fields around three dimensional objects by integral equation methods**  
*J. Sound Vib.*, 1980 Vol. 69. No.1. 71-100.p.
10. Ouellet, D. and Guyader, J.-L.: **Theoretical and experimental study of partial enclosures**  
*Proc. Inter-Noise 88*, 413-416.p.
11. Seybert, A.F., Wu, T.W. and Li, W.L.: **Analysis of noise radiated by a source within a partial enclosure using the Boundary Element Method**  
*Proc. Inter-Noise 89*, 1225-1228.p.
12. Yasuda, H., Matsui, M. et al.: **Noise reduction and sound radiation efficiency of the enclosure for different attachment conditions by airborne sound**  
*Proc. Inter-Noise 83*, 323-326.p.
13. Drozdova, L. Ph.: **New method for calculation and design noise isolating enclosures**  
*Proc. 2nd Int. Cong. Recent Developments in Air- and Structure-borne Sound and Vib.*, 1992, 485-492.p.
14. Thien, G.E.: **The use of enclosures for reducing engine noise.** In: *Engine noise - Excitation, Vibration and Radiation* (Eds.: R. Hickling and M.M.Kamal), Plenum Press, New York - London, 1982, 345-385.p.



15. Beranek, L.L. and Vér, I.L. (Eds.): **Noise and vibration control engineering. Principles and applications**  
John Wiley, New York, 1992, Chapter 13.
16. Verheij, J.W., Hoerberichts, A.N.J. and Thompson, D.J.: **Acoustical source strength characterisation for heavy road vehicle engines in connection with pass-by noise**  
*Proc. Third Int. Cong. on Air- and Structure-borne Sound and Vib.* (Ed.: M.J. Crocker), Montreal, June 13-15 1994. Vol. I. 647-654.p.
17. Augusztinovicz, F. and Sas, P.: **Evaluation and validation of numerical calculation methods for prediction of insertion loss of close-fitting engine enclosures**  
*Proc. Inter-Noise 93* (Ed.: P. Chappelle and G. Vermeir), Leuven, 1993, Vol.II. 721-726.p.
18. Augusztinovicz, F., Sas, P. and Penne, F.: **Sound radiation from structures in the presence of close-fitting sound shields**  
*Proc. Noise-Con 94*, Fort Laudardale, May 1-4 1994, 219-224.p.
19. Augusztinovicz, F., Sas, P. and Penne, F.: **Simulation of shielding of diesel engine noise by means of physical and numerical models**  
*Proc. of the 19th ISMA* (Ed.: P. Sas), Leuven, 1994, Vol II. 825-840.p.
20. **SYSNOISE User Manuals**, Revision 5.0 and 5.1, Numerical Integration Technologies, Leuven, 1993 - 1994.
21. K. De Langhe and P. Sas: **An experimental-analytical SEA identification and applied validation criteria of a box type structure**  
*Proc. of the 19th ISMA* (Ed.: P. Sas), Leuven, 1994, Vol I. 431-446.p.